CONF-8708164--1

PROBING THE VACUUM WITH HIGHLY CHARGED IONS

C. BOTTCHER

Argonne National Laboratory, Argonne IL 60439-4843*

and

M. R. STRAYER

Oak Ridge National Laboratory, Oak Ridge, TN 37831

CONF-8708164--1

DE88 001431

Abstract

The physics of the Fermion vacuum is briefly described, and applied to pair production in heavy ion collisions. We consider in turn low energies (< 50 MeV/nucleon), intermediate energies (< 5 GeV/nucleon), and ultrahigh energies such as would be produced in a ring collider. At high energies, interesting questions of Lorentz and gauge invariance arise. Finally, some applications to the structure of high Z atoms are examined.

*This work supported by the Department of Energy, Office of Basic Energy Sciences, under contract W-31-109-ENG-38.

PS

1. Introduction

In 20th century physics the vacuum has replaced the luminous ether of the Victorians. The Fermion vacuum was introduced by Dirac [1] in the form of a negative energy sea. He observed that the spectrum of a single electron in the field of a nucleus (fig. 1) consisted of a negative energy continuum $E < -mc^2$, as well as the usual bound states and positive energy continuum $E > mc^2$. The ground state does not decay because all the lower states are filled, and transitions are blocked by the Pauli principle. This model predicts pair production under an electromagnetic perturbation. If a negative energy electron is promoted to an empty state $E > -mc^2$, the remaining hole is observable as a positron.

However, care is needed to avoid infinities. If we postulate that the unperturbed vacuum has no observable properties (it is "hairless") then such quantities as ρ_{vac}, the charge density of the vacuum, are unobservable, and indeed they appear in the theory as formally infinite constants. If perturbed by a time dependent electromagnetic field, ρ_{vac} evolves into $\rho(t)$ and that $\rho(t)-\rho_{vac}$ is measurable. A formal apparatus for such calculations is outlined in the next section.

In the past two decades, interest in the vacuum has been spurred by several developments. One was the suggestion by Greiner and his co-workers that pair production could be studied using the electric fields of highly charged ions produced by the GSI accelerators. The electric field at the edge of a uranium nucleus (10^{19} V/cm) is the largest available under laboratory control. Another was the idea of Lee and Wick that, under conditions of high compression, the vacuum of the strong interaction might change dramatically leading to new phases of matter. While the QCD vacuum represents the "holy grail" of present day physics, the QED vacuum is still the place to start testing theoretical ideas. Lastly, but of great importance, we must add the recent

interest in precision measurements using high Z atoms, as represented in other papers in this volume.

In the remainder of this article we shall derive a working set of equations describing the strongly perturbed vacuum. We then illustrate the application of these equations to electron-positron pair production at both high and low energies. Finally, we indicate how they might be applied to the stationary states of high Z ions.

As general references we can recommend two recent edited volumes [2,3].

2. Dirac-Fock equations for the vacuum

We wish to derive a self-consistent set of equations describing a system of electrons and positrons in a strong external field. The electrons and positrons can be treated as independent particles, since their behavior is dominated by the external field, which can be treated classically [4].

Thus we introduce a complete set of states of a one-body Dirac equation

$$H\,\phi_k = E_k\,\phi_k\,(\vec{r}) \tag{2.1}$$

H describes the initial state of the system, and can be determined later. This set is used to define creation operators of physical electrons,

$$a_k^+|0\rangle = |\phi_k^+\rangle = |\phi_k\rangle \quad (E_k>0) \tag{2.2}$$

and

$$b_\ell^+|0\rangle = |\phi_\ell^-\rangle = |\phi_\ell^*\rangle \quad (E_k<0) \tag{2.3}$$

As usual $|0\rangle$ is the vacuum (filled sea). Notice that ϕ_ℓ^- is time-reversed (corresponding to a hole). Statistics are expressed in relations such as

$$\left\{a_k^+ \, , \, a_\ell\right\} = \delta_{k\ell} \tag{2.4}$$

Full details can be found in an ref. [4].

Under a perturbation, a_k and b_k^+ mix according to a Bogoliubov transformation,

$$a_k(t) = \sum_\ell \left(U_{k\ell}\, a_\ell + V_{k\ell}\, b_\ell^+\right)$$

$$b_k^+(t) = \sum_\ell \left(-V_{k\ell}\, a_\ell + U_{k\ell}\, b_\ell^+\right) \tag{2.5}$$

which has the formal property that

$$N = \langle \sum_k a_k^+ \, a_k + \sum_\ell b_\ell \, b_\ell^+ \rangle \tag{2.6}$$

is conserved. N is not the lepton number (pairs can be created!) but rather the total charge, as can be seen using (2.4); in units of (-e)

$$N = \langle \sum_k a_k^+ \, a_k - \sum_\ell b_\ell^+ \, b_\ell + \sum_\ell 1 \rangle \tag{2.7}$$

The three terms are the electronic charge, the positronic charge, and the vacuum charge (an infinite constant). Subtraction of the vacuum properties is always taken care of if the operators in expressions like (2.6) are normally ordered, which we indicate by colons, e.g.

$$: b_\ell \, b_\ell^+ : \; = - \, b_\ell^+ \, b_\ell \tag{2.8}$$

We determine how the system evolves by postulating the Kerman-Koonin action principle [5],

$$\delta S = 0 \tag{2.9}$$

$$S = \int d^4x \langle \Phi(t) | \; : L(x) : \; | \Phi(t) \rangle \tag{2.10}$$

L(x) is the operator Lagrangean density, and $|\Phi(t)\rangle$ the state vector of the many-particle system. The Lagrangean has parts describing the electromagnetic field, the fermion fields, and the external field interaction,

$$\begin{aligned} L(\chi) = & -\frac{1}{4} F_{\mu\nu} F^{\mu\nu} \\ & - \psi(\chi) \{\gamma_0 \gamma^\mu (p_\mu + A_\mu) - m\} \psi(\chi)^+ \\ & - J_\mu^{ext} A^\mu \end{aligned} \tag{2.11}$$

In the independent particle model

$$|\Phi(t)\rangle = \prod_{0<k<F} a_k^+ |0\rangle \tag{2.12}$$

where the product runs over particles in the Fermi sea. It is often more convenient to write a_k^+ in terms of Schwinger operators, which create a particle at a point,

$$a_k^+ = \int d^3\vec{r} \; \phi_k(\vec{r}t) \; \psi(\vec{r})^+ \tag{2.13}$$

If S is stationary with respect to A_μ, we must have,

$$\boxed{} A_\mu = J_\mu^{ext} + \psi \gamma_0 \gamma_\mu \psi^+ \tag{2.14}$$

Thus A_μ has in addition to A_μ^{ext}, a part

$$A_\lambda^{scf}(\chi) = \int d^{3+}y \; D_{\lambda\mu}\,(\chi-y)\,\left[\psi\,\gamma_0\gamma^\mu\psi(y)^+\right] \tag{2.15}$$

where D is the photon propagator (or Green's function of $\Box$). When (2.15) is inserted in (2.11), the Lagrangean acquires an e-e interaction term,

$$\int L_I d^{3+}x = \frac{1}{2}\int d^{3+}x d^{3+}y \; D\lambda_\mu(x-y)\,\left[\psi\gamma_0\gamma^\lambda\psi(\chi)^+\right]\,\left[\psi\gamma_0\gamma^\mu\psi(y)^+\right] \tag{2.16}$$

Combining (2.9)-(2.16) and varying all the Fermion fields, we arrive at the following equations:

$$i\,\frac{\partial\phi_k}{\partial t} = \sum_\ell H[k,\ell]\;\phi_\ell \tag{2.17}$$

where $\{\phi_k\}$ includes the occupied electron states $0<k<F$, and all the vacuum states $k<0$.

For $k<0$, ϕ_k corresponds to the negatron state generated by b_k, rather than the positron state generated by b_k^+. The operator H is readily expressed using the shorthand notation,

$$V = \gamma_0\gamma^\mu A_\mu = A_0 - \vec{\alpha}\cdot\vec{A} \tag{2.18}$$

thus

$$H[k,\ell] = \delta_{k\ell}\left\{\vec{\alpha}\cdot\vec{p} + \beta m + V^{ext} + \sum_q{}' \; V[q,q]\right\}$$

$$- V[k,\ell] \tag{2.19}$$

The second term -V[k,ℓ] is the exchange (Fock) term, while

$$V^{dir} = \sum_q{}' \; V[q,q] \tag{2.20}$$

is the direct (Hartree) term. The potentials in V are obtained from the

Fermion currents through

$$\boxed{} A_\mu[k,\ell] = J_\mu[k,\ell] = \phi_k^* \gamma_0 \gamma_\mu \phi_\ell(\chi) \tag{2.21}$$

For the direct term (2.20), a subtraction must be performed, as indicated by the prime on the summation,

$$\sum_q{}' J_\mu[q,q|t\}] = \sum_{0<q<F} J_\mu[q,q|t]$$

$$+ \sum_{q<0} \{J_\mu[q,q|t] - J_\mu[q,q|0]\} \tag{2.22}$$

The second term is negative (in units of -e) corresponding to the positron current.

Stationary solutions of (2.17) correspond to

$$\phi_k(\chi) = \exp(-i\epsilon_k t)\ \vec{\phi}_k(\vec{r}) \tag{2.23}$$

Then (2.21) becomes (letting $\epsilon_k - \epsilon_\ell = \omega_{k\ell}$)

$$(\omega_{k\ell}^2 - \nabla^2)\ A_\mu[k,\ell] = \vec{\phi}_k^* \gamma_0 \gamma_\mu \vec{\phi}_\ell(\vec{r}) \tag{2.24}$$

Thus the direct terms ($k = \ell$) are generated by the unretarded Coulomb interaction.

Subsequent sections will examine applications of (2.17)-(2.22).

3. The diving model of pair production

Collisions of very heavy ions (e.g. U + Cm) at slow to intermediate energies (say $0.1 < \beta < 0.9$) appear at first sight formidably complicated. Yet it is possible to describe pair production in these systems in terms of a tractable model. In the notation of (2.19), let $\{\phi_k\}$ be the stationary and $\{\psi_k(t)\}$ the

time dependent solutions, such that

$$\psi_k(-\infty) = \phi_k \quad (k < F) \tag{3.1}$$

Then the probability of creating a pair $E(e^-) = \epsilon_k$, $E(e^+) = |\epsilon_\ell|$ is given by

$$P_{k\ell} = |\langle\phi_k|\psi_\ell(\infty)\rangle|^2 \tag{3.2}$$

If, as is the case for colliding, slow heavy ions, the largest term of the type (3.2) is $k = 0$ $[1s_{1/2}]$, then it is simpler to invoke time reversal, and calculate

$$P_{\ell 0} = |\langle\phi_\ell|\psi_0(\infty)\rangle|^2 \tag{3.3}$$

In words, this formula expresses the diving of a $1s_{1/2}$ hole into the negatron continuum, as illustrated in fig. 1. For a very slow collision, one may think of the hole spontaneously decaying into the vacuum.

In practical terms we can drop all interelectron terms in (2.17) as compared to the nuclear potentials. Then pair production (3.2) can be calculated by solving [6]

$$[H_T + V_P(t)]\ \psi = i\,\frac{\partial\psi}{\partial t} \tag{3.4}$$

where H_T is the target Hamiltonian and V_P the perturbation induced by the projectile. For slow ions (say $\beta < 0.2$), it is further possible to approximate V_P by its leading monopole term [6], reducing (3.4) to a radial Dirac equation. In customary notation, ψ is replaced by a two-component object, satisfying

$$i\,\frac{\partial}{\partial t}\begin{bmatrix} G(r) \\ F(r) \end{bmatrix} = \begin{bmatrix} mc^2 + V & \frac{\partial}{\partial r} + \frac{k}{r} \\ -\frac{\partial}{\partial r} + \frac{k}{r} & -mc^2 + V \end{bmatrix} \begin{bmatrix} G \\ F \end{bmatrix} \tag{3.5}$$

The assumptions of the diving and monopole approximations may seem arbitrary at first sight, but they are better appreciated by looking at the numerical behavior of the K-shell orbital in heavy ions. The length scales involved are illustrated in fig. 2. An unperturbed K-shell has a radius of ~ 10^3 fm, while the nuclear radius ~ 10 fm. However, if two nuclei with a combined charge $\gtrsim$ 170 are brought within 50 fm, the 1s orbital collapses to ~ 100 fm, i.e. within the Compton wavelength $\lambda\!\!\!^{-}_{\ell}$ = 386 fm. The energy eigenvalue of the collapsed orbital lies in the negative energy continuum, which is not surprising, since the potential energy of an electron at a distance $\lambda\!\!\!^{-}_{\ell}$ from the united nucleus ~ $-2mc^2$. The diving and monopolar assumptions are thus justified by the energy and radius of the 1s orbital, respectively.

Figure 3 shows the G and F components of the 1s orbital of Cf, and of the combined U + Cf system at a separation of 42 fm, the distance at which $\epsilon(1s) \simeq -mc^2$. One observes the contracted radius, and the enhanced F component, suggesting a large overlap with the negative energy continuum. It is instructive to look at the momentum wave functions. Figure 4 shows the momentum distributions, for positive and negative energies, in the Cm 1s state. The mean momentum of the positive energy component ~ 0.68 mc, but the negative energy component is pushed much further out (~ 1.27 mc) and it has a long tail. These distributions account for many features observed in pair production.

We shall now look in more detail at the specific case of U + Cm collisions at 6.05 MeV/nucleon, for which good data exist [2]. The positron singles spectrum has been observed in coincidence with nuclear scattering between 25° and 65° in the laboratory; this corresponds to distances of closest approach between 19 fm and 30 fm, for which diving is probable. The positron spectrum is a broad hump, peaking around 600 keV, and extending to ~ 1200 keV. In

round numbers, one positron is produced for every 10^5 collisions, corresponding to a total cross section of 170 μb. The probability of producing a positron is the product of the probabilities for generating a K-shell hole (~ 0.05) and for filling that hole by the diving mechanism (~ 2×10^{-4}).

In fig. 5 we show the results of solving (3.5) for these collisions [6]. The positron spectrum in fig. 5a is in good agreement with the experiments, both in shape and absolute magnitude. Figures 5b-5d show the effect on the spectrum of introducing increasing nuclear time delays at the distance of closest approach. The broad hump evolves into a sharp peak at ~ 300 keV. These time delays were an early model to explain the sharp "anomalous" peak observed in some experiments. The model was abandoned because no justification for delays > 10^{-21} second could be found in nuclear physics.

4. Anomalous positron and electron peaks

As series of papers [7] have appeared describing sharp peaks in e^+ and e^- singles spectra, and in coincidence, at approximately 180°. The experiments in question are again those involving heavy ions at low energies. All attempts to explain the phenomena have so far failed. They cannot be nuclear, since the peak energies are independent of nuclear charge and energy. Theories involving a resonance a in $e^+ + e^-$ scattering [8] also fail,

$$U + Cm \rightarrow e^+ + e^- \leftrightarrow [a] \qquad (4.1)$$

since no such resonance is known. Searches in regions of mass and lifetime allowed by known data in particle physics and QED have proved negative [9].

Even if some a was found, a process such as (4.1) would still be difficult to reconcile with elementary two-body kinematics. If we write the momentum of a as

$$\vec{P} = \vec{p}_+ + \vec{p}_- \qquad (4.2)$$

the experiments (sharp singles peaks) require that $P \lesssim$ [illegible] MeV/c while p_+, $p_- \sim$ 300 MeV/c. These constraints cannot be satisfied without additional ad hoc assumptions.

It must be pointed out that the conditions of the heavy ion experiments are unhappily ideal for producing artifacts closely resembling the observed peaks. They use thick targets in conjunction with large angle detectors. Thus, annihilation gamma rays can produce copious Compton and photoelectronic edges in the range 200-400 keV, which are difficult to distinguish kinematically from genuine e^+ or e^- peaks. More precise, and probably very difficult experiments, are required to establish the reality of the anomalous peaks, before more theoretical efforts can be justified.

5. Pair production at intermediate heavy ion velocities $0.4 < \beta < 0.98$

We have investigated the general features of heavy ion collisions in the energy range 0.1-4 GeV/nucleon, using another one-dimensional model distinct from the radial model of sec. 3. At these velocities, a fully Lorentz invariant formulation is required. Most dynamics will take place along the direction of Lorentz contraction, so that a reduction to one cartesian dimensional ought to describe a head-on collision, qualitatively at any rate [3,4].

The Dirac equation has two components, as in sec. 3, but (3.5) is replaced by

$$i \frac{\partial}{\partial \tau} \begin{bmatrix} G(x) \\ F(x) \end{bmatrix} = \begin{bmatrix} m - A_0 & -\frac{\partial}{\partial x} - iA_x \\ \frac{\partial}{\partial x} + iA_x & -m - A_0 \end{bmatrix} \begin{bmatrix} G(x) \\ F(x) \end{bmatrix} \qquad (5.1)$$

The covariant potentials are given by

$$A_0 = - V_T(\chi) - \gamma V_P [\gamma(\chi-\beta t)] \tag{5.2}$$

$$A_x = \gamma\beta V_P [\gamma(\chi-\beta t)] \tag{5.3}$$

where the target (T) is at rest, and the projectile (P) has velocity β (in units of the speed of light). We represent the target and projectile by cutoff Coulomb fields,

$$V_N = - \frac{Q_N}{(x^2 + a_N^2)^{1/2}} \quad (N = P,T) \tag{5.4}$$

The parameters were chosen to mock up a U + Cm collision, and the diving model was used for pair production. Further details of the calculations are given in refs. [3] and [4].

The calculations consisted of following the time evolution of a particle (or hole) initially localized in the 1s state of the target. The projectile is bare. The wave function at a large time was then projected on complete sets of target and projectile states, in accordance with (3.3). In figs. 6 and 7, we show the time evolution of G and F for $\beta = 0.4$ and 0.98 respectively. At low velocities, capture occurs into the 1s state of the target, almost adiabatically. At very high velocities, little evidence of capture is seen, but F has a large component moving with and ahead of the projectile. This suggests that energetic positrons might be observed in the forward direction, at ion energies of a few GeV/nucleon. The evidence of fig. 7 is confirmed by the calculated projections [3], and we refer to these as "snow plough" positrons. In a sense, they are the analogue of the familiar "convoy" electrons, which trail behind the projectile.

Figure 8 shows some final state probabilities. The total inelastic probability below 1 GeV/nucleon is dominated by K-K capture, and peaks around $\beta = 0.6$, as one might have predicted from fig. 4. Positron production hovers around 10% for most of the range studied. If this probability is converted to a cross section, using $\pi\lambda\!\!\!^{-2}$ as a geometric scale, where $\lambda\!\!\!^{-}$ is the Compton wavelength, we get ~ 100 b for pair production at 1 GeV/nucleon. At higher energies, different mechanisms take over, as we shall see in the following section.

6. Pair production at ultrahigh energies

To focus this section, some experimental background is useful. Heavy ion storage rings are under construction or proposed in laboratories around the world. The most ambitious is the Relativistic Heavy Ion Collider (RHIC) at Brookhaven. Suppose two heavy ions (e.g. U + U) collide head on, each having energy $E_c = \gamma_c Mc^2$ in the laboratory. The equivalent fixed-target energy is then $E = \gamma Mc^2$, where

$$\gamma = 2\gamma_c^2 - 1 \qquad (6.1)$$

e.g. an E_c = 100 GeV/nucleon, as proposed for RHIC, results in E = 20,400 GeV/nucleon. This arithmetic has consequences for electromagnetic pair production, since the operative quantity here is the transverse electric field produced by one nucleus, seen from the other nucleus,

$$E_\perp \sim \alpha Z\gamma/b^2 \qquad (6.2)$$

Thus we expect prolific pair production not only of $e^\pm$, but of the heavier leptons $\mu^\pm$ and $\tau^\pm$. Since $m_\mu = 206.77$ and $m_\tau = 3491.6$ in units of m_e, their Compton wavelengths are 1.87 and 0.11 fm respectively. We should therefore expect that the heavier particles would be produced inside the nucleus, or even inside the nucleon!

Extensive formal discussions of pair production by external fields are available in textbooks [10]. However, they are not well suited to calculations on strong fields, and they cover over some serious theoretical problems, as we shall indicate shortly. We shall proceed using the concepts illustrated in fig. 1. In contrast to low energy collisions, transitions are predominantly from the vacuum to the positive energy continuum. Bound states are of small importance. The rate of pair production is obtained by adapting (3.2) and (3.4). The Dirac equation becomes

$$[\vec{\alpha}\cdot(\vec{p}-\vec{A}_p) + \beta m_\ell - \phi_p - \phi_T]\ \psi = i\,\frac{\partial\psi}{\partial t} \tag{6.3}$$

where m_ℓ is the lepton mass, and the target is stationary. Then we begin in a negative energy state of given momentum and spin,

$$\psi_i(-\infty) = \phi^-(\vec{k}_i s_i) \tag{6.4}$$

The probability of producing a lepton pair

$$(-\vec{k}_i - s_i,\ \vec{k}_f s_f)$$

is then

$$P_{if} = |\langle\phi^+(\vec{k}_f s_f)|\psi_i(\infty)\rangle|^2 \tag{6.5}$$

If momentum normalizations are used, the rate of pair production is

$$N = (2\pi)^{-3}\int d^3\vec{k}_i \int d^3\vec{k}_f\ P_{if} \tag{6.6}$$

A question at once arises, to which we have no simple answer. Since the initial eigenstate is un-normalized, how is pair production suppressed at large distances? The problem is more tractable if the projectile is replaced by a transverse electromagnetic pulse ($\beta \simeq 1$),

$$\phi = f[\gamma(t-z)] \tag{6.7}$$

$$\vec{A} = \vec{e}_x \phi \tag{6.8}$$

For a point nucleus,

$$f(s) = -\frac{aZ_T\gamma}{(b^2+s^2)^{1/2}} \tag{6.9}$$

This model may be solved in perturbation theory, leading to the famous Weizsäcker-Williams virtual photon model [11].

The first order expression for (6.5) is

$$P_{if} = \left| \int dt \, \exp(i\omega_{if}t) \, \langle i|V_p|f\rangle \right|^2 \tag{6.10}$$

where the kets are target eigenstates. The leading term in (6.10) gives a pair production cross section

$$\sigma_{pp} = \int_{\omega_0}^{\omega_1} d\omega_{if} \, \frac{4Z_P^2}{\gamma^2} \, |\langle i|\alpha_x|f\rangle|^2 \int_{b_1}^{\infty} 2\pi b db K_1\left(\frac{\omega_{if} b}{\gamma}\right) \tag{6.11}$$

This equivalent to the Weizsäcker-Williams expression

$$\sigma_{pp} = \int_{\omega_0}^{\omega_1} d\omega \, F(\omega) \, Q_T(\omega) \tag{6.12}$$

where F is the flux of virtual photons and Q_T the $\gamma + T \to \ell^- + \ell^+ + T$ cross section. The choice of cutoffs ω_0, ω_1 and b_1 is rather tricky.

The matrix element $\langle i|\alpha_x|f\rangle$ is in fact proportional to Z_T, so that the process is really second order, involving scattering by both projectile and target nuclei. At very high energies ($\gamma > 100$), (6.12) reduces to

$$\sigma_{WW} = \frac{28}{27\pi} (\alpha Z_p Z_T)^2 \lambda_\ell^2 (\ell n \gamma)^3 \qquad (6.13)$$

The assumptions leading to (6.12) are questionable for the heavy leptons. A complete solution of (6.3)-(6.5) is not yet possible, so we have initiated another approach, using an effective local field model. The formal theory of pair production suggests that the process is rather localized in space and time, so that the number of pairs produced by a set of electromagnetic fields has the form [12]

$$N = \int d^3\vec{r}dt \; W(E^2-B^2, \vec{E}\cdot\vec{B}) \qquad (6.14)$$

This is the most general local expression which is Lorentz and gauge invariant. In the case of a collision, it is necessary to subtract terms arising from the target or projectile alone. The leading terms are then quadratic in $E^2 - B^2$ and $\vec{E}\cdot\vec{B}$.

We have constructed approximations to the function W using perturbation theory and a soluble (Schwinger) model

$$\phi = 0, \; \vec{A} = \vec{e}_x a(t) \qquad (6.15)$$

Some results are indicated in fig. 9, where we plot the cross sections for $e^\pm$, $\mu^\pm$ and $\tau^\pm$ predicted by our model vs. collider (i.e. laboratory) energy. The following numbers are in order.

(i) At very high energies, any model of the form (6.14) $\sigma \sim \ell n\gamma$, in contrast to (6.13). The discrepancy between our model and Weizsäcker-Williams is indeed $\sim (\ell n\gamma)^2$. There is agreement around 1 GeV.

(ii) The τ cross sections are larger than predicted from a point nucleus theory. The τ^+ is produced at the center of the target, and hence sees no Coulomb repulsion.

(iii) For a luminosity of 10^{27} $cm^{-2}s^{-1}$, as projected by RHIC, a 1 mb cross section gives 1 count per second. Thus, allowing for uncertainties in our models, we expect 1-10 $\mu^{\pm}/s$ and 0.1-1 $\tau^{\pm}/s$ at RHIC. We also estimate that a heavier lepton of mass ~ 100 m_τ would be just detectable.

7. The structure of highly charged ions

We have mostly been concerned with dynamical problems, but it is interesting to ask whether the method outlined in sec. 2 might usefully be applied to problems of atomic structure. One possibility would be the structure of ions with $Z > 137$.

The eq. (2.19), with the vacuum coupled in, contains some effects usually attributed to QED, e.g. part of the vacuum polarization. The Uehling potential arises from the density of electrons in the negative energy sea, a they are perturbed by the nucleus,

$$V_1(r) = \int \frac{\delta\rho(\vec{s})}{|\vec{r}-\vec{s}|}\, d^3\vec{s} \tag{7.1}$$

where

$$\delta\rho = \sum_{q<0} |\phi_q(\vec{r})|^2 - \rho_0 \tag{7.2}$$

where ρ_0 is chosen to make the integral over $\delta\rho$ vanish. Preliminary calculations of V_1 are encouraging. If V_1 is inserted back in the equations for ϕ_q, so that the vacuum is determined self-consistently, effects of higher order in $Z\alpha$ are obtained.

Suppose we wish to go beyond Dirac-Fock. If two electronic orbits i, j, are excited from the Fermi sea, the energy is corrected by Rayleigh-Schrödinger perturbation theory

$$\Delta E^{(2)} = \sum_{a,b} \frac{\langle ij|v|ab\rangle}{\epsilon_i + \epsilon_j - \epsilon_a - \epsilon_b} , \qquad (7.3)$$

where v is some residual interaction. If we ignore the vacuum, ϵ_a can be large and positive, and ϵ_b large and negative in such fashion that the denominator in (7.3) vanishes. This is the Brown-Ravenhall disease [13]. In our formulation, the vacuum states are excluded from the sum by the Pauli principle, so the disease is cured. The price is that double excitations from the vacuum must be calculated. This program has not yet been carried through.

Appendix

Numerical methods

We shall here briefly mention the numerical method used to obtain many of the results quoted in the text, particularly in sec. 5. This is the "basis spline collocation method". Fuller details are given in ref. [3] and particularly ref. [4].

Suppose we wish to solve

$$\left[-\frac{1}{2}\frac{d^2}{dx^2} + V(x) \right] \psi(x) = E\psi(x) \qquad (A.1)$$

in terms of the values ψ_α of $\psi(x)$ at a set of points ξ_α. These are the collocation points. We expand $\psi(x)$ in a set of basis splines,

$$\psi(x) = \sum_{k=1}^{u} \psi^k u_k(x) \qquad (A.2)$$

Each u_k is a piecewise continuous polynominal of order (N-1), localized at a set of points $\{x_k \ldots x_{k+N}\}$ referred to as knots (fig. 10). For N odd, the collocation points are then halfway between the knots

$$\xi_\alpha = \frac{1}{2}\,(\chi_{\alpha+\mu} + \chi_{\alpha+\mu+1}) \quad , \quad \mu = (N-1)/2 \tag{A.3}$$

The collocation method requires that (A.1) is satisfied identically at the collocation points,

$$-\frac{1}{2}\sum \psi^{k} u_k''(\xi_\alpha) + V_\alpha \psi_\alpha = E\psi_\alpha \tag{A.4}$$

If ψ_k is eliminated by solving

$$\psi_\alpha = \sum \psi^{k} u_k(\xi_\alpha) \tag{A.5}$$

we arrive at our discrete representation of (A.1),

$$\sum_\beta (T_{\alpha\beta} + V_\alpha\, \delta_{\alpha\beta})\, \psi_\beta = E\psi_\alpha \tag{A.6}$$

Local operators such as V are thus represented by diagonal matrices.

The power of these methods is illustrated by fig. 11, which plots the error in a certain quantity (the ground state energy in a Morse potential) vs. the number of mesh points. For high order polynominals, the error decreases very rapidly. Thus high accuracy is attained with only a modest number of points.

References

[1] P. A. M. Dirac, "Quantum Mechanics", Oxford Univ. Press (Clarendon), London (1957).

[2] "Quantum Electrodynamics of Strong Fields", ed. W. Greiner, Plenum Press, New York (1983).

[3] C. Bottcher and M. R. Strayer, in Proceedings of the Atomic Theory Workshop on "Relativistic and QED Effects in Heavy Atoms", Gaithersburg, Maryland, May 1985, AIP Conf. Proc. No. 136, Am. Inst. of Phys., New York (1985).

[4] C. Bottcher and M. R. Strayer, Ann. Phys. (NY) 175 (1987) 64.

[5] A. K. Kerman and S. E. Koonin, Ann. Phys. (NY) 100 (1976) 332.

[6] C. Bottcher and M. R. Strayer, Phys. Rev. Lett. 54 (1985) 669.

[7] T. Cowan, H. Backe, M. Beremann, K. Bethge, H. Bokemeyer, H. Folger, J. S. Greenberg, H. Grein, A. Gruppe, Y. Kido, M. Kluver, D. Schwalm, J. Schweppe, K. E. Steibing, N. Trautmann and P. Vincent, Phys. Rev. Lett. 54 (1985) 1761; M. Clemente, E. Berdermann, P. Kienle, H. Tsertos, W. Wagner, C. Kozhuharov, F. Bosh and W. Koening, Phys. Lett. B 137 (1984) 41.

[8] A. B. Balantekin, C. Bottcher, M. R. Strayer and S. J. Lee, Phys. Rev. Lett. 55 (1985) 461; A. Schafer, J. Reinhardt, B. Muller, W. Greiner and G. Soff, J. Phys. G 11 (1985) 169; W. Lichten and A. Robatino, Phys. Rev. Lett. 54 (1985) 781.

[9] K. A. Erb, I. Y. Lee and W. T. Milner, Phys. Lett. B 181 (1986) 52.

[10] C. Itzykson and J.-B. Zuber, "Quantum Field Theory", McGraw-Hill, New York (1980).

[11] W. Heitler, "Quantum Theory of Radiation", Oxford Univ. Press (Clarendon), London (1954).

[12] J. Schwinger, Phys. Rev. 82 (1951) 664.

[13] C. Bottcher and M. R. Strayer, in Proceedings of the "NATO International Advanced Course on Physics of Strong Fields", Maratea, Italy, June 1986 (in press).

[14] G. E. Brown and E. G. Ravenhall, Proc. Roy. Soc. (London), A208 (1951) 552.

Figure captions

Fig. 1 Energy spectrum of particle and hole states for an electron in the field of a heavy nucleus. The arrows S and D distinguish schematically the spontaneous and dynamical mechanism of positron production.

Fig. 2 Length scales in a collision between two heavy ions: (a) nuclear radius; (b) electron Compton wavelength; (c) radius of uranium K-shell.

Fig. 3 G and F components of the $1s_{1/2}$ wave function are plotted as a function of distance from the center of the Cf nucleus for A: Cf alone; B: Cf + U at a distance of 42 fm; C: indicates the Cf nuclear radius. G and F are shown as full and dotted lines, respectively.

Fig. 4 Momentum distributions for the positive (full line) and negative (dotted line) energy components of the 1s orbital of Cm. The vertical scale is linear in arbitrary units.

Fig. 5 U + Cm head-on collision at a bombarding energy of 6.05 MeV per particle. The spectrum is expressed as $dP/d\epsilon$, the probability per mc^2, per collision, of producing a single positron or electron. Positron (full line) and electron (dotted line) spectra in the target frame, for (a): no time delay; (b), (c), (d) respectively T = 2.5, 5, 20 $\alpha^2 t_0$ (1.21×10^{-21}s).

The positron spectrum for b = 19 fm is shown by the dashed line in (a). In (d) the arrows A,B indicate the peak position in a head-on U + Pu collision, and a U + Cm collision at b = 19 fm (both at the same bombarding energy.

Fig. 6 U(P) + Cm(T) collision in a one-dimensional model at a projectile velocity 0.4 c (85 MeV/nucleon). The $|G|^2$ and $|F|^2$ components of the particle density are plotted vs. distance along the internuclear axis (in units of Compton wavelength) as full and dashed lines respectively. The passage of time in the three frames is indicated by the advance of P from left to right. The vertical scale is linear in arbitrary units.

Fig. 7 Same as fig. 7, for a projectile velocity 0.98 c (3.8 GeV/nucleon).

Fig. 8 Combined final-state probabilities for the target and projectile frames as functions of the projectile velocity: (in) total inelastic; (e^-) positive energy continuum (electrons); (e^+) negative energy continuum (positrons). The dashed line is an estimate of the proportional error in the numerical procedures.

Fig. 9 Pair production cross sections vs. projectile or target energy in a collider for electrons, muons, and tauons. Full curves refer to U + U, and dashed to Kr + Kr collisions. W is our calculation of e^- production from a Weizsäcker-Williams model divided by one hundred.

Fig. 10 Quadratic (third order) basis spline. The knots are indicated by the filled circles and the collocation points by the open circles.

Fig. 11 Error analysis of the ground-state eigenvalues of a model Hamiltonian described in ref. [4]. We plot log (calculated-exact) vs. $\log_2$ (number of lattice points) for four methods: full line, N = 3 splines; dotted line, N = 5 splines; dashed line, N = 7 splines; dot-dashed line, finite-difference.

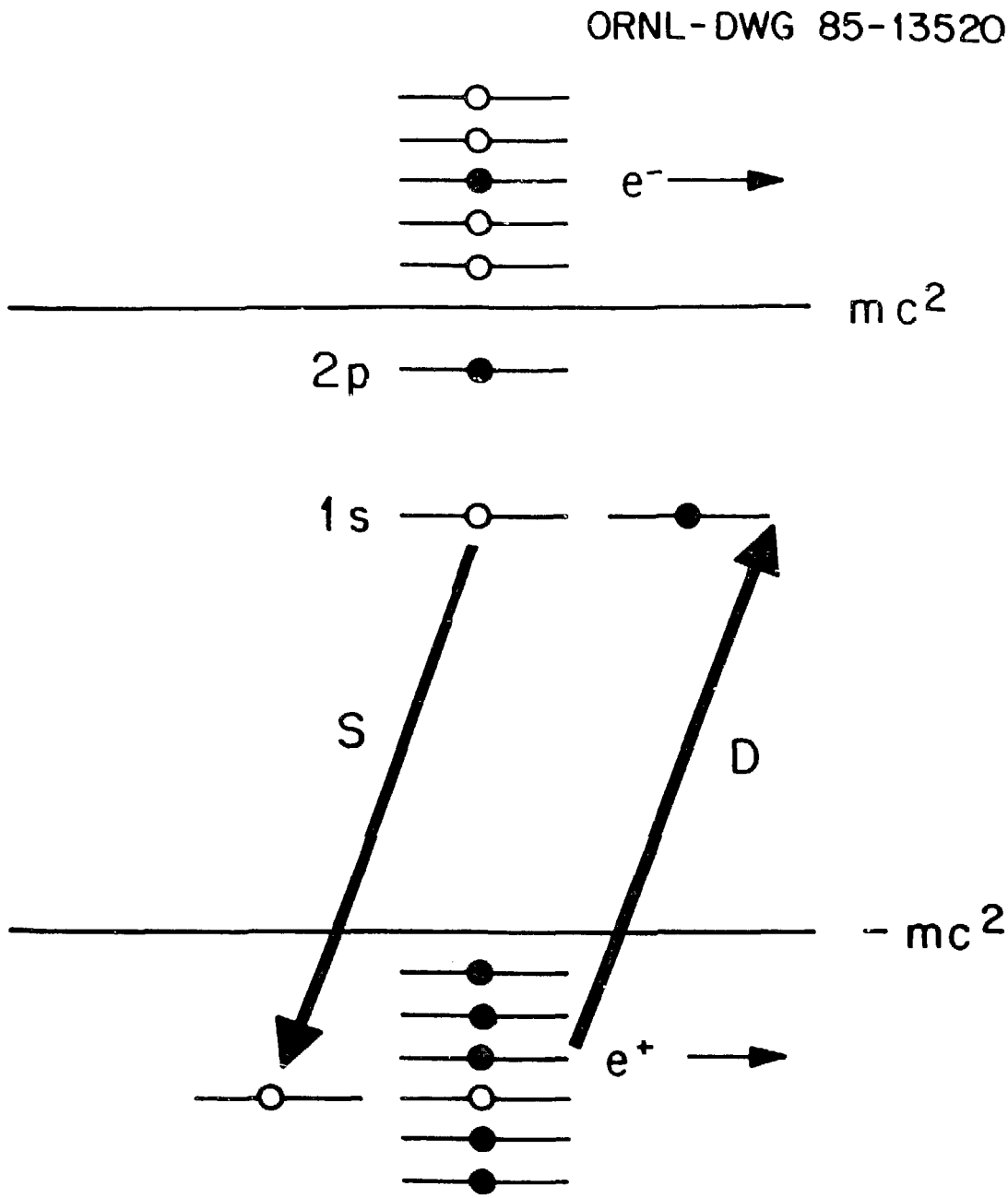

Fig. 1

ORNL-DWG 85-13532

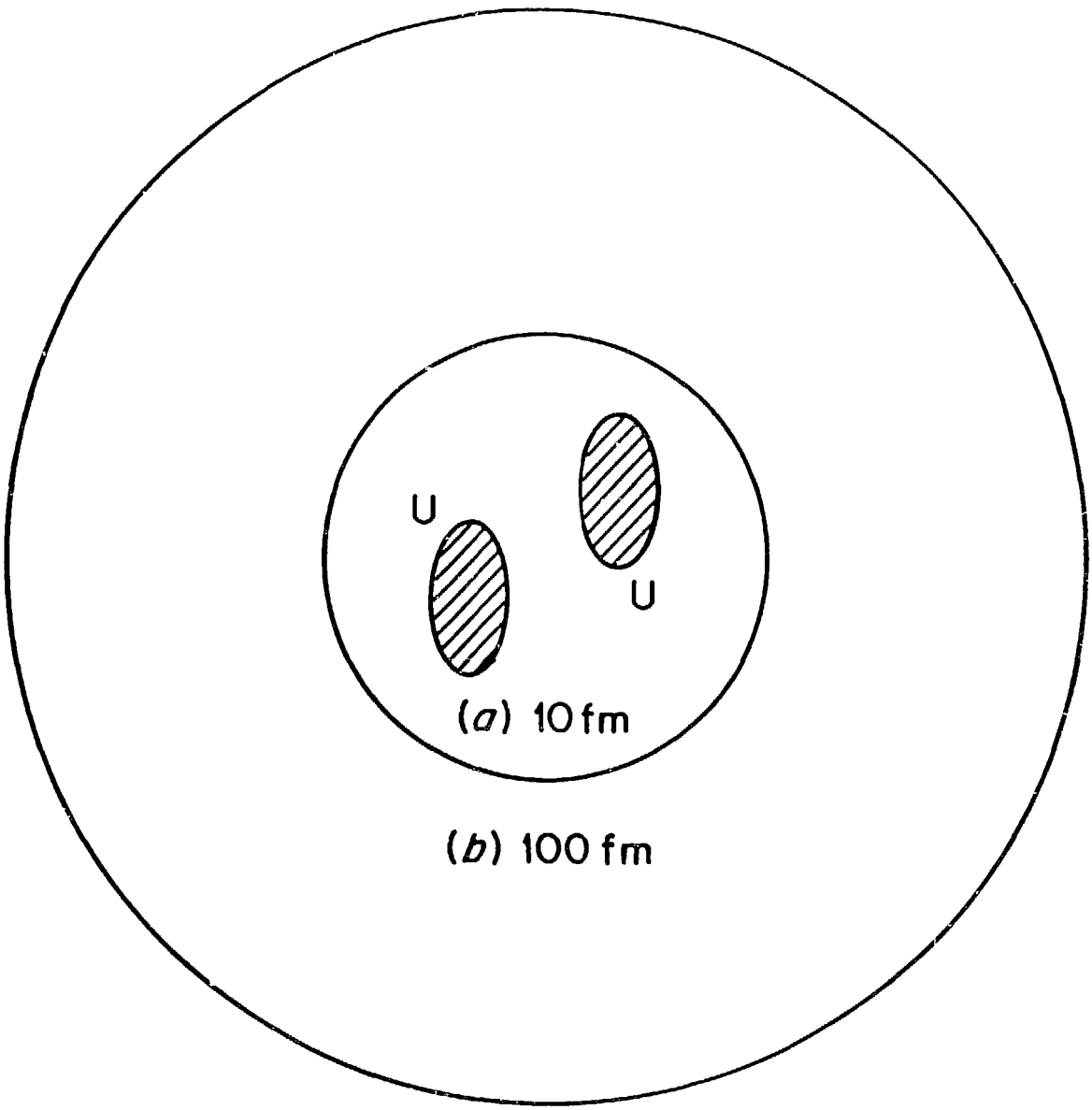

Fig. 2

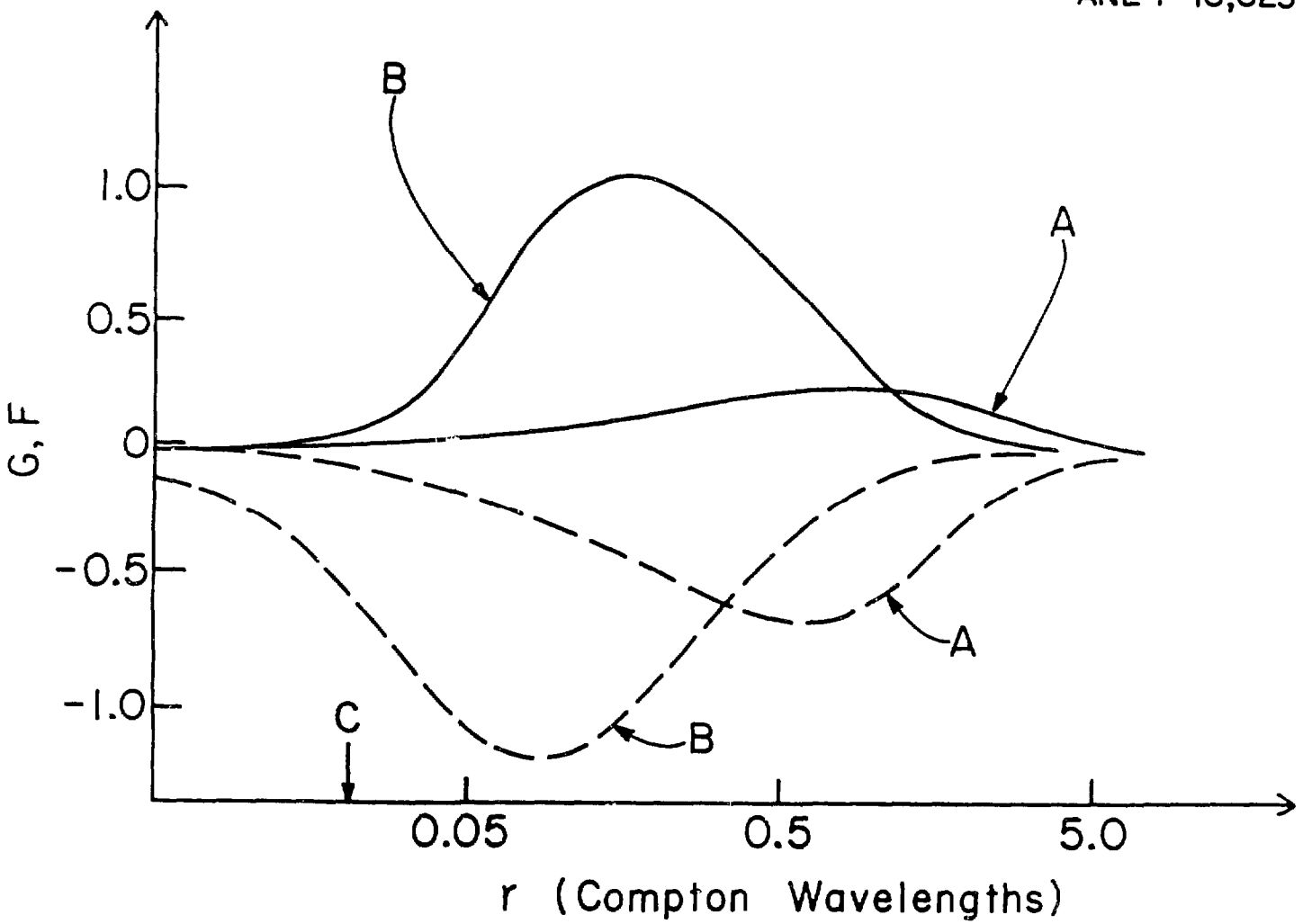

Fig. 3

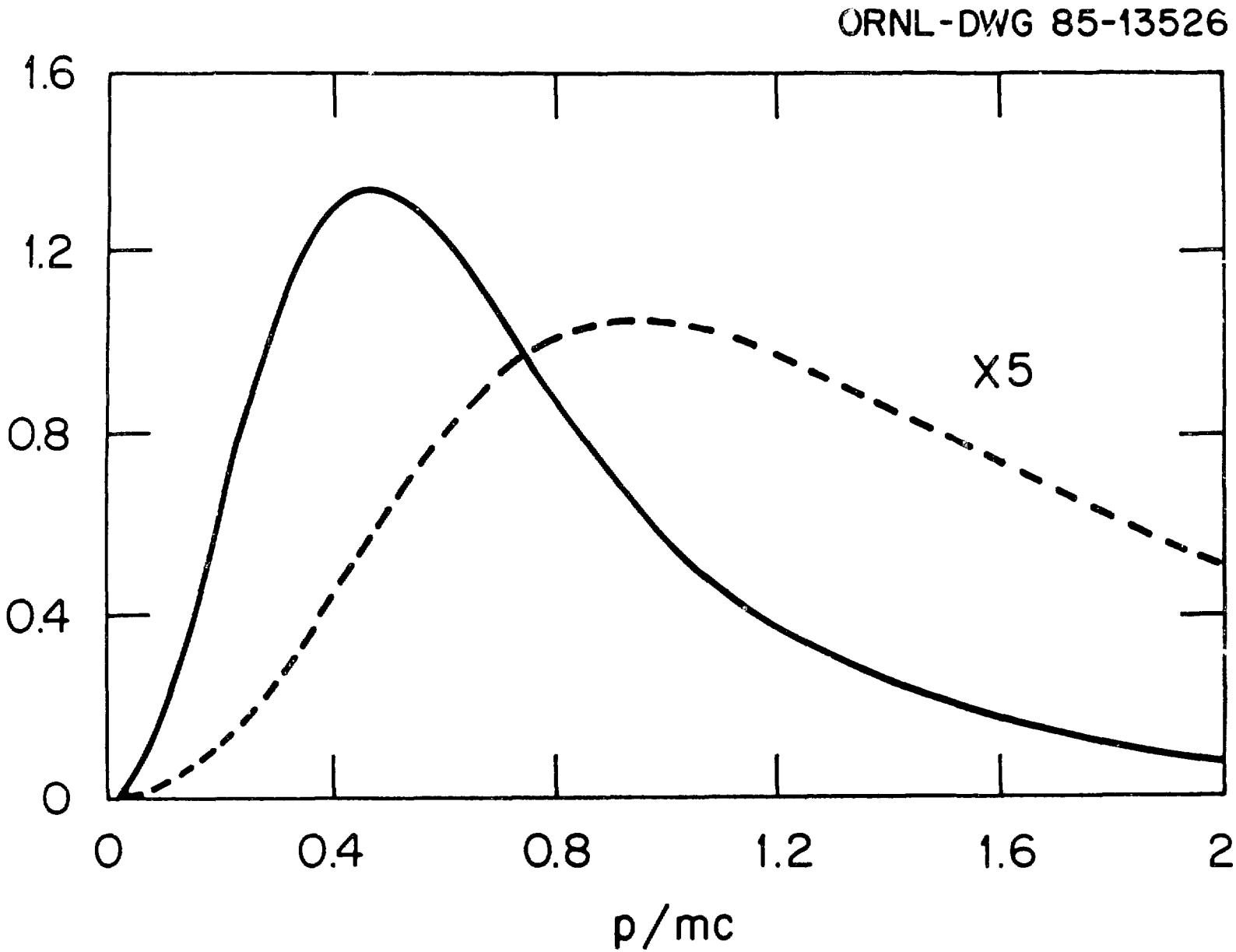

Fig. 4

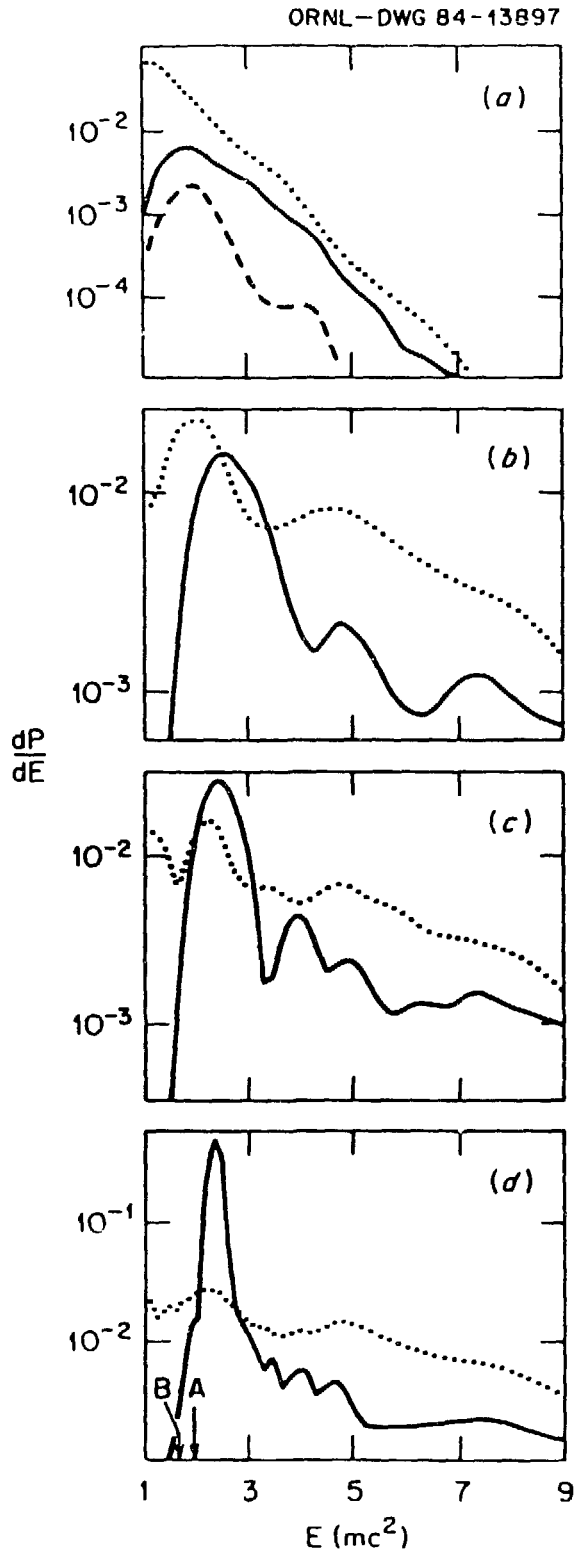

Fig. 5

ORNL-DWG 85-13528

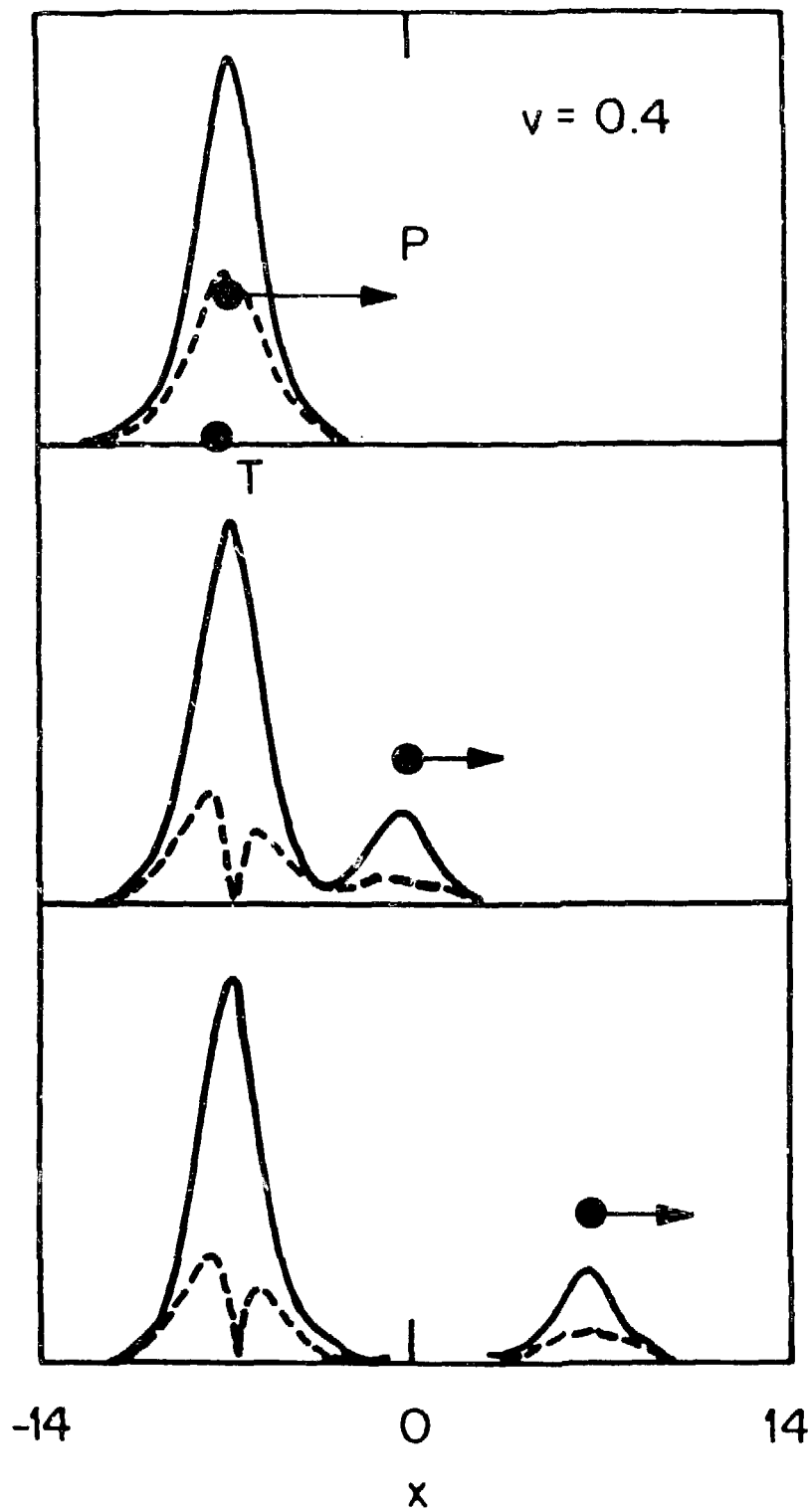

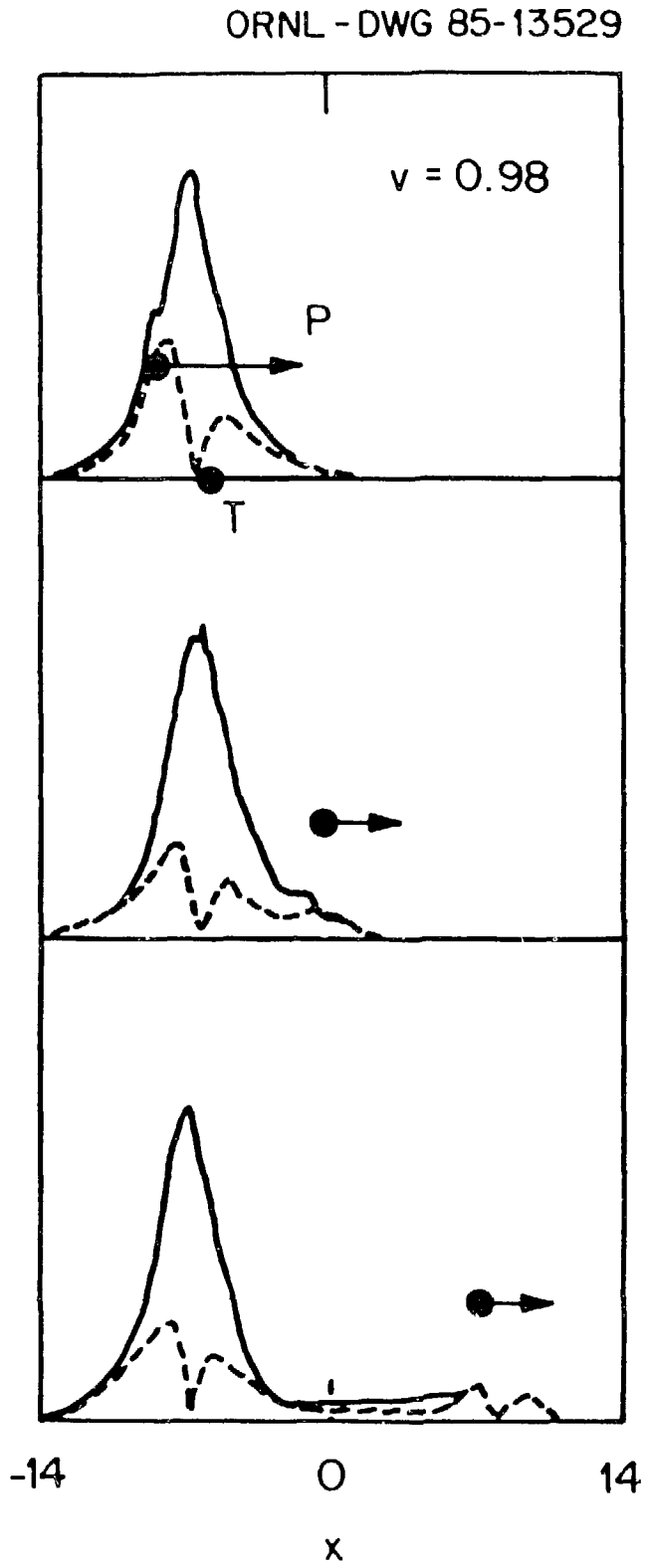

Fig. 7

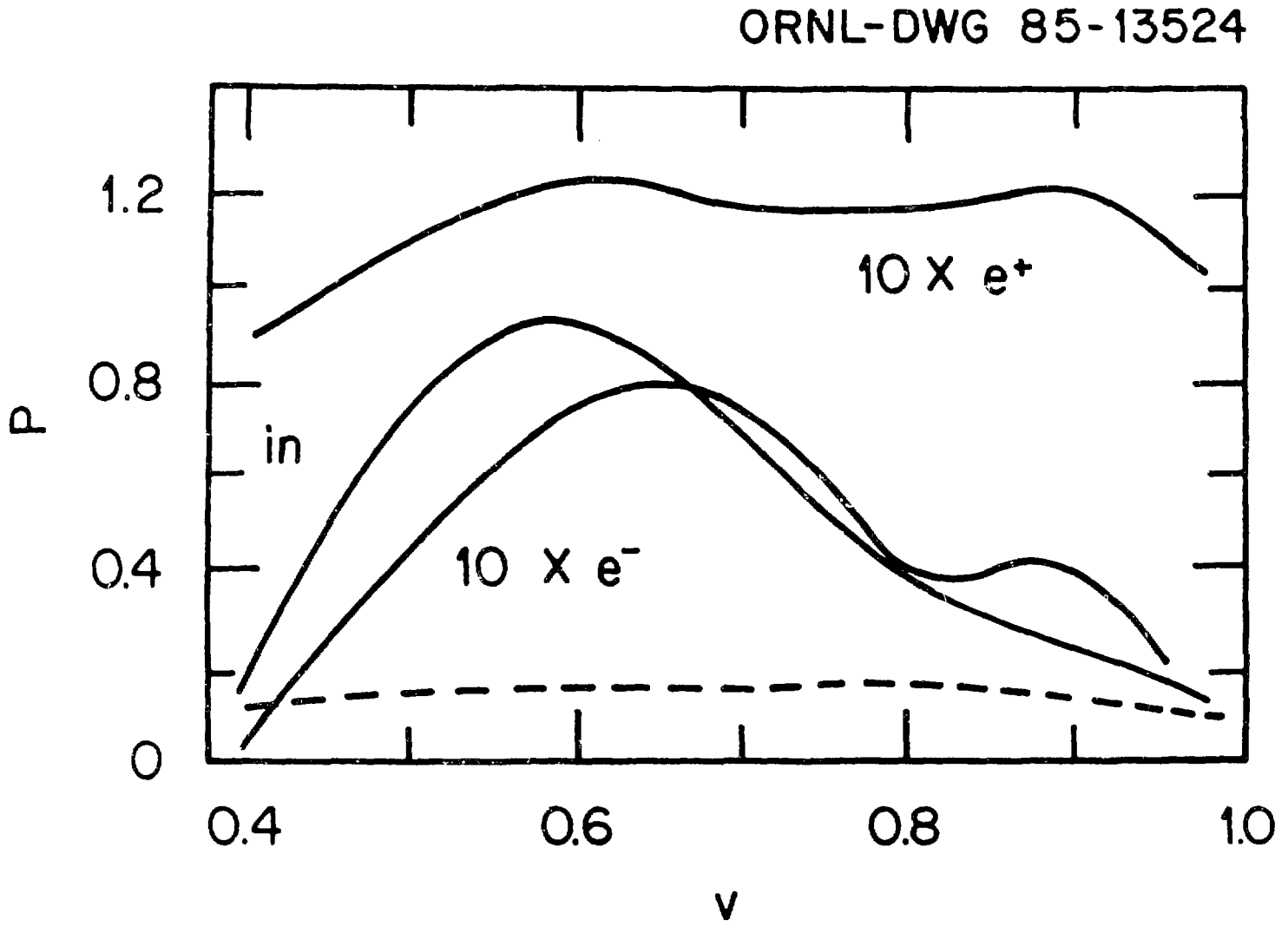

Fig. 8

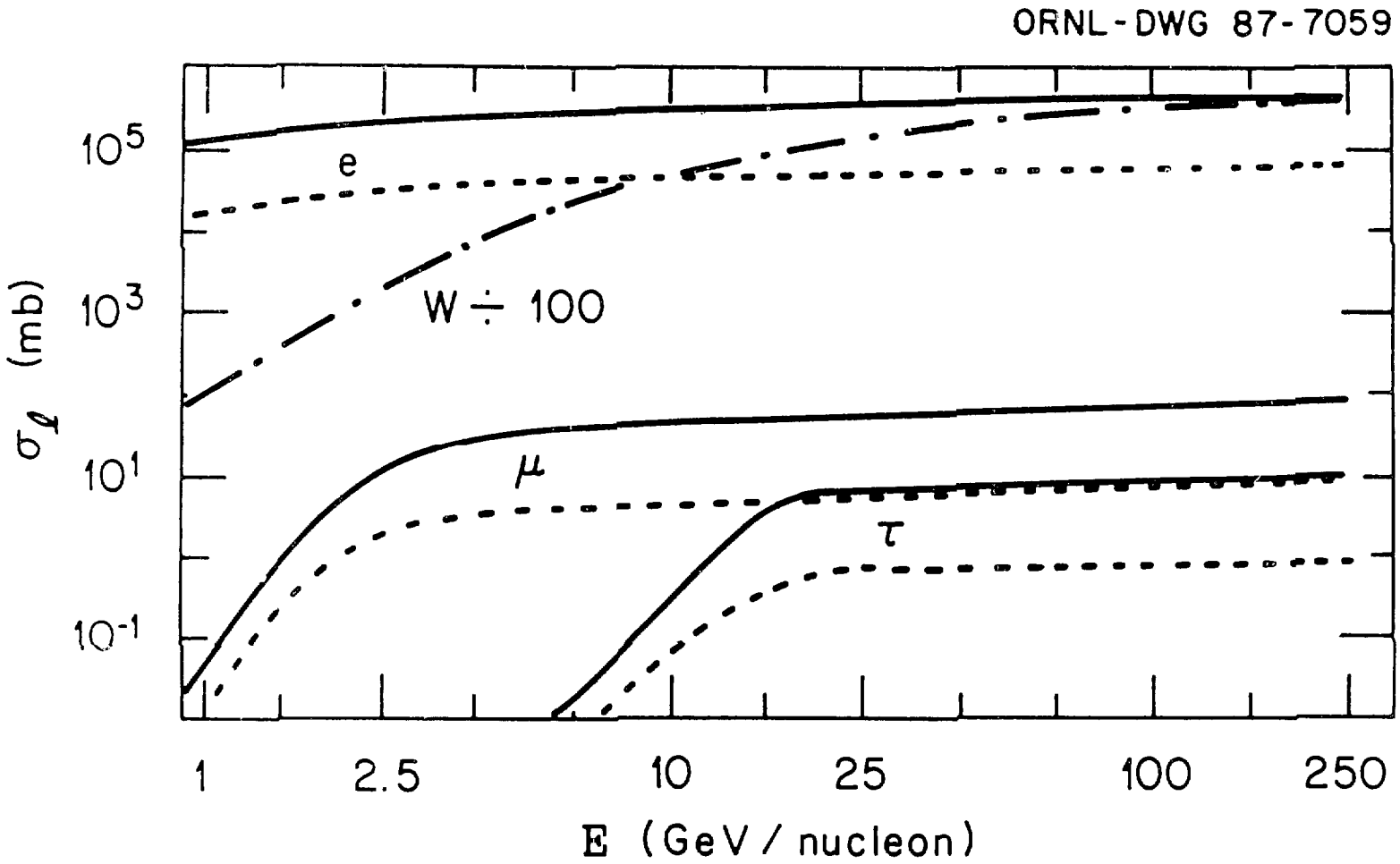
ORNL-DWG 87-7059
10^5
10^3
10^1
10^{-1}
σ_ℓ (mb)
e
W ÷ 100
μ
τ
1
2.5
10
25
100
250
E (GeV / nucleon)

Fig. 9

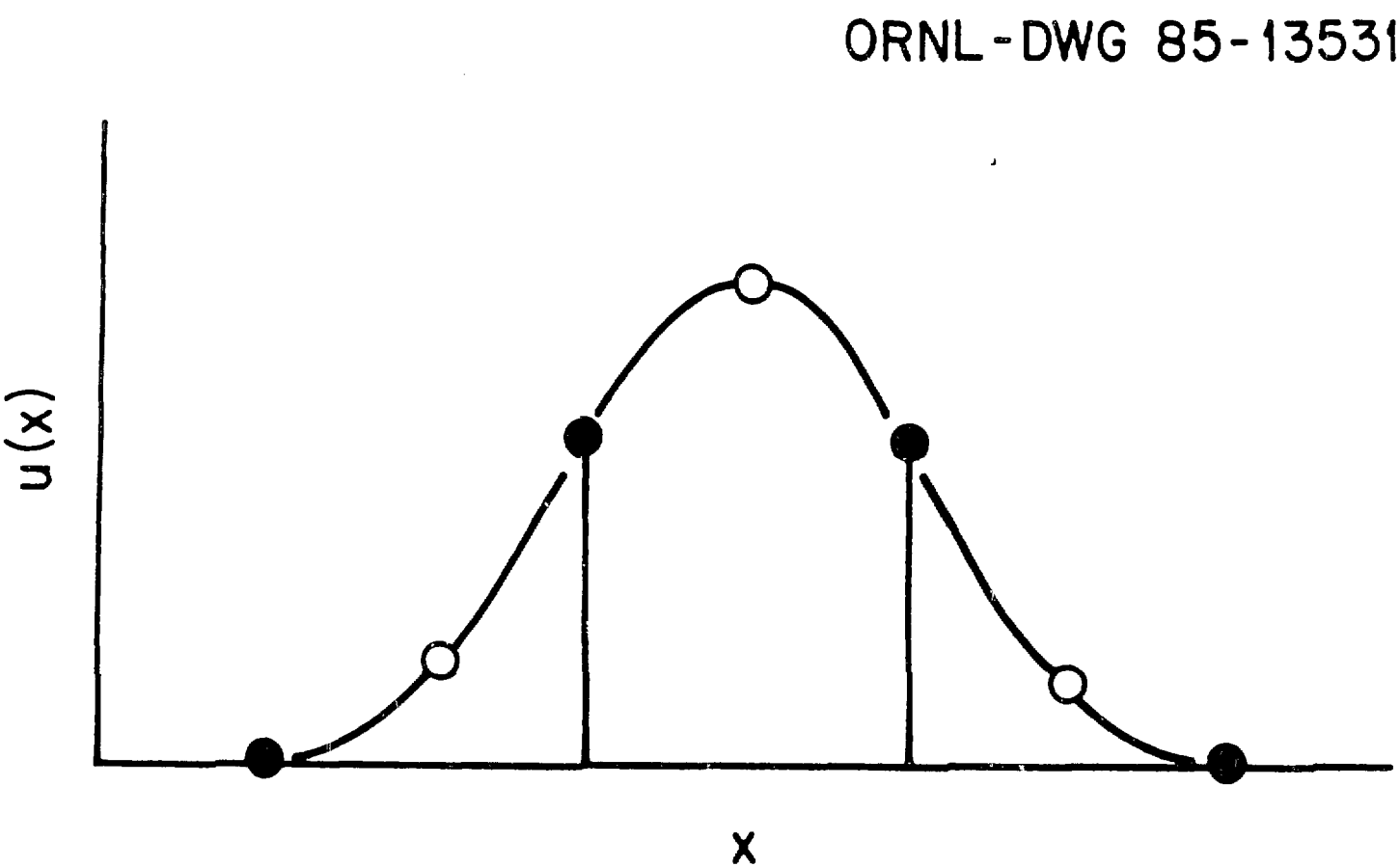

Fig. 10

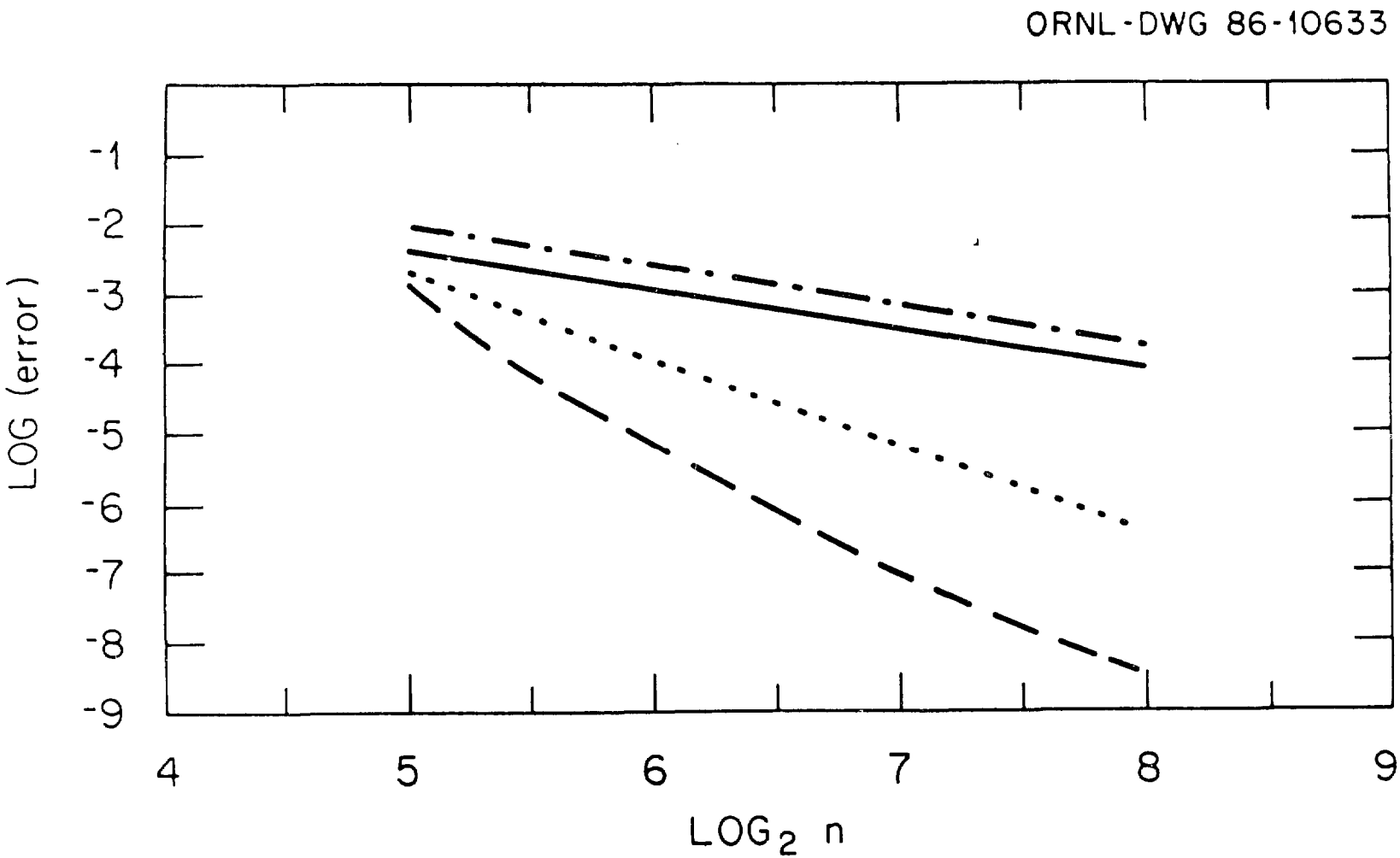

Fig. 11